Computers and Structures 182 (2017) 419–429

Contents lists available at ScienceDirect

Computers and Structures

journal homepage: www.elsevier.com/locate/compstruc

An iterative algebraic dynamic condensation method and its performance

Seung-Hwan Boo, Phill-Seung Lee *

Department of Mechanical Engineering, Korea Advanced Institute of Science and Technology, 291 Daehak-ro, Yuseong-gu, Daejeon 34141, Republic of Korea

ARTICLE INFO

Article history:
Received 12 September 2016
Accepted 29 December 2016

Keywords:
Finite element method
Structural dynamics
Reduced-order modeling
Iterated improved reduced system method
Algebraic substructuring

ABSTRACT

A novel iterative reduced-order modeling method is proposed, which is based on the recently developed algebraic dynamic condensation method. The algebraic substructuring technique is employed to improve the reduction efficiency, and the initial reduced model is calculated using the substructural stiffness condensation and the interface boundary reduction procedures. Then, the initial reduced model is iteratively updated using the iterative substructural inertial effect condensation procedure until the solutions converge. The iterative formulation of the reduced model is represented simply with small submatrix operations to avoid huge computational cost induced by the iterative procedure resulting from the very large global transformation matrix. To verify the performance of the proposed method, we consider several large structural problems, and compare the numerical results to those of the iterated improved reduced system (IIRS) method, a widely used reduced-order modeling method.

1. Introduction

While computational resources have been greatly improved, the demand for dynamic analysis of large and complex structural systems, which are modeled using the finite element (FE) method, has increased even more rapidly. Because dynamic analysis using global size matrices can be very time-consuming work, dynamic condensation methods [1–11] have been widely used for several decades. The reduced-order models obtained via dynamic condensation methods are very important in a number of research fields, including structural health monitoring, structural design optimization, multi-body dynamics, FE model updating, and experimental-FE model correlation [12–22].

The pioneering work for dynamic condensation methods is the static condensation method proposed by Guyan [2] and Irons [3] in the 1960 s. In 1989, O'Callahan [5] developed the improved reduced system (IRS) method employing the newly derived transformation matrix. This is calculated by adding the extra term containing inertial effect to Guyan's transformation matrix [2]. Since then, there have been considerable efforts to improve the solution accuracy of the IRS method. Friswell [7] developed the iterative IRS transformation matrix, and proposed the iterated IRS (IIRS) method. After that, Xia and Lin [8] proposed the modified IIRS transformation matrix, and improved the convergence speed of the IIRS method. To improve the computational efficiency of the Guyan, IRS, and IIRS methods, there have been several studies [23–28] employing physical domain based substructuring, which is a key concept of the component mode synthesis (CMS) methods [29–37].

Because the formulations of the IRS and IIRS methods are simple and produce accurate reduced models, those methods have been widely used. However, the IRS and IIRS methods have a critical limitation to handle very large FE models with hundreds of thousands of degrees of freedom (DOFs). This is because the part of the transformation matrix corresponding to the truncated DOFs is highly populated, which induces huge computational cost. Considering the recent trend of increase in the size of FE models, it is very important to overcome this limitation of the IRS and IIRS methods.

Recently, to resolve the limitation of the IRS method, we developed a very efficient and accurate method, which is named "algebraic dynamic condensation method" [1], exploiting the algebraic substructuring technique [38–43]. It was reported that the algebraic dynamic condensation method could handle a very large FE model with hundreds of thousands of DOFs, which could not be solved using the IRS method, and that the performance of this method was much superior to the IRS method in terms of both the solution accuracy and computational efficiency.

In this study, as an extension of the algebraic dynamic condensation method [1], a new iterative reduced-order modeling method is proposed. Using the algebraic substructuring technique [38], the global mass and stiffness matrices are automatically partitioned into small submatrices. To construct an initial reduced model,

* Corresponding author.
E-mail address: phillseung@kaist.edu (P.-S. Lee).

http://dx.doi.org/10.1016/j.compstruc.2016.12.011
0045-7949/

the substructural stiffness is condensed into the interface boundary, and the interface boundary is reduced using the dominant interface normal modes. Then, the initial reduced model is iteratively updated until satisfying the designated error tolerance through the iterative substructural inertial effect condensation procedure. To reduce computational cost, the formulation of the iterative reduced model is expressed by simple multiplications and summations of small submatrices. The performance of the proposed method is verified considering several large structural FE models. It is observed that the computational efficiency of the proposed method is much superior to that of the IIRS method, with more accurate solutions. Furthermore, the proposed method can handle large FE models that the IIRS method cannot handle.

In the following sections, the formulation of the IIRS method is reviewed briefly, and the proposed method is derived. We then evaluate the performance of the proposed method compared to that of the IIRS method using several structural problems. Finally, conclusions are drawn.

2. Iterated IRS (IIRS) method

In structural dynamics, the equations of motion for un-damped free vibration without damping are given by

$$\mathbf{M}_g\ddot{\mathbf{u}}_g + \mathbf{K}_g\mathbf{u}_g = \mathbf{0}, \tag{1}$$

where $\mathbf{M}_g$ and $\mathbf{K}_g$ are the global mass and stiffness matrices, respectively, and $\mathbf{u}_g$ is the global displacement vector. In the IIRS method, before reducing the global system, the global matrices and vector are separated as

$$\mathbf{M}_g = \begin{bmatrix} \mathbf{M}_t & \mathbf{M}_{tr} \\ \mathbf{M}_{tr}^T & \mathbf{M}_r \end{bmatrix}, \ \mathbf{K}_g = \begin{bmatrix} \mathbf{K}_t & \mathbf{K}_{tr} \\ \mathbf{K}_{tr}^T & \mathbf{K}_r \end{bmatrix}, \ \mathbf{u}_g = \begin{bmatrix} \mathbf{u}_t \\ \mathbf{u}_r \end{bmatrix}, \tag{2}$$

in which the subscripts t and r denote the truncated and retained DOFs, respectively, and the subscript tr denotes the coupled DOFs between t and r.

The global eigenvalue problem is defined by

$$\mathbf{K}_g\mathbf{u}_g = \lambda\mathbf{M}_g\mathbf{u}_g, \tag{3}$$

and its partitioned form is expressed as

$$\begin{bmatrix} \mathbf{K}_t & \mathbf{K}_{tr} \\ \mathbf{K}_{tr}^T & \mathbf{K}_r \end{bmatrix}\begin{bmatrix} \mathbf{u}_t \\ \mathbf{u}_r \end{bmatrix} = \lambda\begin{bmatrix} \mathbf{M}_t & \mathbf{M}_{tr} \\ \mathbf{M}_{tr}^T & \mathbf{M}_r \end{bmatrix}\begin{bmatrix} \mathbf{u}_t \\ \mathbf{u}_r \end{bmatrix}, \tag{4}$$

in which λ denotes the eigenvalue of the global system.

Expanding the first row in Eq. (4), the truncated DOFs vector $\mathbf{u}_t$ is written as

$$\mathbf{u}_t = -\mathbf{K}_t^{-1}\mathbf{K}_{tr}\mathbf{u}_r + \lambda\mathbf{K}_t^{-1}(\mathbf{M}_{tr}\mathbf{u}_r + \mathbf{M}_t\mathbf{u}_t). \tag{5}$$

Assuming a transformation matrix $\mathbf{T}$ between $\mathbf{u}_t$ and $\mathbf{u}_r$, the truncated DOFs vector $\mathbf{u}_t$ is rewritten as

$$\mathbf{u}_t = \mathbf{T}\mathbf{u}_r. \tag{6}$$

Substituting Eq. (6) into $\mathbf{u}_t$ in the right-hand side of the Eq. (5), the following equation is obtained

$$\mathbf{u}_t = [-\mathbf{K}_t^{-1}\mathbf{K}_{tr} + \lambda\mathbf{K}_t^{-1}(\mathbf{M}_{tr} + \mathbf{M}_t\mathbf{T})]\mathbf{u}_r, \tag{7}$$

and from the relation $\mathbf{u}_t = \mathbf{T}\mathbf{u}_r$ in Eq. (6), the transformation matrix $\mathbf{T}$ can be defined as

$$\mathbf{T} = \mathbf{T}_s + \lambda\mathbf{K}_t^{-1}(\mathbf{M}_{tr} + \mathbf{M}_t\mathbf{T}) \ \text{ with } \mathbf{T}_s = -\mathbf{K}_t^{-1}\mathbf{K}_{tr}. \tag{8}$$

Using the transformation matrix $\mathbf{T}$ in Eq. (8), the global displacement vector $\mathbf{u}_g$ is represented by

$$\mathbf{u}_g = \begin{bmatrix} \mathbf{u}_t \\ \mathbf{u}_r \end{bmatrix} = \begin{bmatrix} \mathbf{T} \\ \mathbf{I}_r \end{bmatrix}\mathbf{u}_r = (\mathbf{T}_G + \lambda\mathbf{T}_a)\mathbf{u}_r \ \text{ with } \mathbf{T}_G = \begin{bmatrix} \mathbf{T}_s \\ \mathbf{I}_r \end{bmatrix}, \quad \mathbf{T}_a = \begin{bmatrix} \mathbf{K}_t^{-1}(\mathbf{M}_{tr} + \mathbf{M}_t\mathbf{T}) \\ \mathbf{0} \end{bmatrix}, \tag{9}$$

where $\mathbf{T}_G$ is the Guyan transformation matrix [2], which is sometimes called the "static condensation matrix", $\lambda\mathbf{T}_a$ is an additional transformation matrix containing the inertial effects of the truncated DOFs, and $\mathbf{I}_r$ is the identity matrix for the retained DOFs.

Considering only $\mathbf{T}_G$ in Eq. (9), the global displacement vector $\mathbf{u}_g$ is approximated as

$$\mathbf{u}_g \approx \bar{\mathbf{u}}_g = \mathbf{T}_G\mathbf{u}_r, \tag{10}$$

and applying Eq. (10) into Eq. (3), the following reduced eigenvalue problem is obtained

$$\bar{\mathbf{K}}_G\mathbf{u}_r = \bar{\lambda}\bar{\mathbf{M}}_G\mathbf{u}_r \quad \text{with } \bar{\mathbf{M}}_G = T_G^{\mathrm{T}}\mathbf{M}_g\mathbf{T}_G, \ \bar{\mathbf{K}}_G = \mathbf{T}_G^T\mathbf{K}_g\mathbf{T}_G, \tag{11}$$

in which $\bar{\mathbf{M}}_G$ and $\bar{\mathbf{K}}_G$ are the reduced mass and stiffness matrices in the Guyan reduction, and $\bar{\lambda}$ is the approximated eigenvalue.

Pre-multiplying $\bar{\mathbf{M}}_G^{-1}$ to Eq. (11), we can obtain the following equation

$$\bar{\lambda}\mathbf{u}_r = \mathbf{H}_G\mathbf{u}_r \ \text{ with } \mathbf{H}_G = \bar{\mathbf{M}}_G^{-1}\bar{\mathbf{K}}_G. \tag{12}$$

In Eq. (9), using $\bar{\lambda}$ instead of λ, and considering the relation $\bar{\lambda}\mathbf{u}_r = \mathbf{H}_G\mathbf{u}_r$ in Eq. (12), the approximated global displacement vector $\bar{\mathbf{u}}_g$ is redefined as

$$\bar{\mathbf{u}}_g = \mathbf{T}_1\mathbf{u}_r \ \text{ with } \mathbf{T}_1 = \begin{bmatrix} \mathbf{T} \\ \mathbf{I}_r \end{bmatrix}, \ \mathbf{T} = \mathbf{T}_s + \mathbf{K}_t^{-1}(\mathbf{M}_{tr} + \mathbf{M}_t\mathbf{T})\mathbf{H}_G. \tag{13}$$

Note that it is not possible to directly calculate the transformation matrix $\mathbf{T}_1$, because the matrix $\mathbf{T}$ is implicit in the formulation. Therefore, an iterative scheme needs to be employed to calculate the transformation matrix $\mathbf{T}_1$.

Employing an iterative scheme, we can define an iterative transformation matrix $\mathbf{T}_1^{(k)}$ as

$$\mathbf{T}_1^{(k)} = \begin{bmatrix} \mathbf{T}^{(k)} \\ \mathbf{I}_r \end{bmatrix} \text{ with } \mathbf{T}^{(k)} = \mathbf{T}_s + \mathbf{K}_t^{-1}(\mathbf{M}_{tr} + \mathbf{M}_t\mathbf{T}^{(k-1)})\mathbf{H}^{(k-1)} \ \text{ for } k \geqslant 2, \tag{14}$$

in which

$$\mathbf{H}^{(k-1)} = (\bar{\mathbf{M}}^{(k-1)})^{-1}\bar{\mathbf{K}}^{(k-1)}, \bar{\mathbf{M}}^{(k-1)} = (\mathbf{T}_1^{(k-1)})^T\mathbf{M}_g\mathbf{T}_1^{(k-1)}, \bar{\mathbf{K}}^{(k-1)} = (\mathbf{T}_1^{(k-1)})^T\mathbf{K}_g\mathbf{T}_1^{(k-1)}, \tag{15a}$$

$$\mathbf{T}^{(1)} = \mathbf{T}_s, \mathbf{H}^{(1)} = \mathbf{H}_G, \mathbf{T}_1^{(k)} = \mathbf{T}_G, \bar{\mathbf{M}}^{(1)} = \bar{\mathbf{M}}_G, \bar{\mathbf{K}}^{(1)} = \bar{\mathbf{K}}_G, \tag{15b}$$

where the superscript k denotes the k^{th} iteration, and when $k = 2$, $\mathbf{T}_1^{(k)}$ is equivalent to the transformation matrix of the improved reduce system (IRS) method [5].

Thus, using the transformation matrix $\mathbf{T}_1^{(k)}$ in Eq. (14), the reduced mass and stiffness matrices in the IIRS method are obtained by

$$\bar{\mathbf{M}}_g = (\mathbf{T}_1^{(k)})^T\mathbf{M}_g(\mathbf{T}_1^{(k)}), \ \bar{\mathbf{K}}_g = (\mathbf{T}_1^{(k)})^T\mathbf{K}_g(\mathbf{T}_1^{(k)}), \tag{16}$$

and the reduced eigenvalue problem is given by

$$\bar{\mathbf{K}}_g(\bar{\boldsymbol{\varphi}})_\mathbf{i} = \bar{\lambda}_\mathbf{i}\bar{\mathbf{M}}_g(\bar{\boldsymbol{\varphi}})_\mathbf{i} \quad \text{for } i = 1, 2, \cdots, N_r, \tag{17}$$

where $\bar{\lambda}_i$ and $(\bar{\boldsymbol{\varphi}})_i$ are the approximated eigenvalues and eigenvectors in the IIRS method, respectively, and N_r is the number of the retained DOFs. Herein, the i^{th} approximated global eigenvector $(\bar{\boldsymbol{\varphi}}_g)_i$ can be calculated by $(\bar{\boldsymbol{\varphi}}_g)_i = \mathbf{T}_1^{(k)}\bar{\boldsymbol{\varphi}}_i$.

It is important to note that, when a large size FE model (over 10^5 DOFs) is considered, the IIRS method could induce a huge computational cost due to a highly populated matrix $\mathbf{T}$ in Eq. (13) requiring large computer memory, which is updated through the iterative procedure to construct the iterative

transformation matrix $\mathbf{T}_1^{(k)}$. Furthermore, the computational cost to calculate the $\bar{\mathbf{M}}_g$ and $\bar{\mathbf{K}}_g$ in Eq. (16) might become high, because three matrices of global DOFs size, $\mathbf{M}_g$ and $\mathbf{K}_g$ ($N_g \times N_g$ matrices), and $\mathbf{T}_1^{(k)}$ ($N_g \times N_r$ matrix), should be handled in the computation. These facts will be investigated using numerical examples in Section 4.

3. Iterative algebraic dynamic condensation method

In this section, we present a new efficient iterative model reduction algorithm, named the iterative algebraic dynamic condensation method. Based on the algebraic dynamic condensation method [1], an iterative substructural inertial effect condensation procedure is newly derived.

3.1. Algebraic substructuring

As shown in Fig. 1, the original global mass and stiffness matrices of the structural FE model are generally large sparse matrices. Using algebraic substructuring [38], the global matrices are automatically permuted. Then, from the algebraic perspective, the permuted matrices can be partitioned into many submatrices corresponding to the substructures and the interface boundary.

Note that, because the matrix permutation is just a simple renumbering process in FE models, the physical characteristic of the original FE models is not altered.

Considering the global mass and stiffness matrices, $\mathbf{M}_g$ and $\mathbf{K}_g$, partitioned into n substructures and the interface boundary by the algebraic substructuring, the global eigenvalue problem is represented by

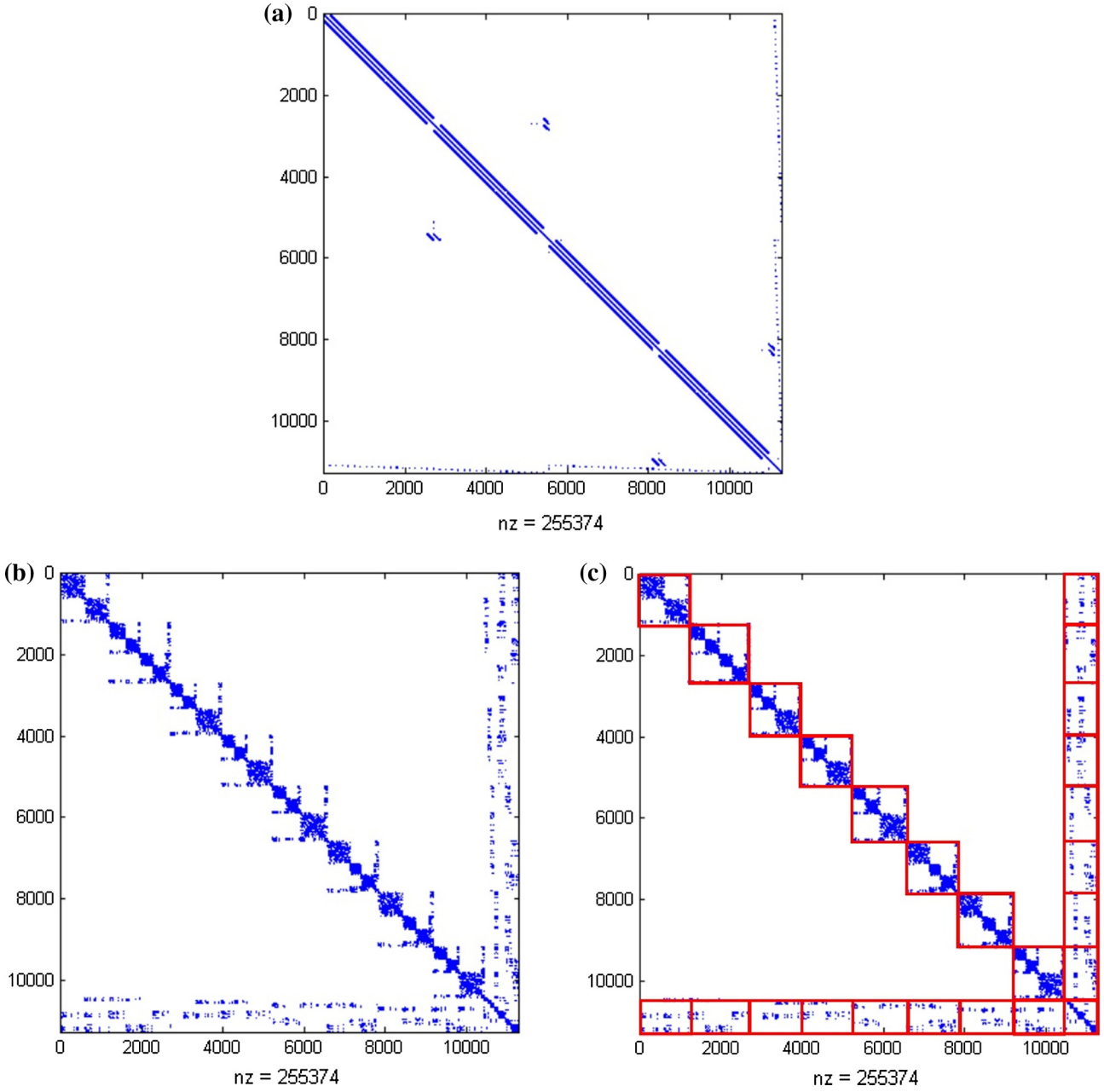

Fig. 1. Algebraic substructuring procedure: (a) original large sparse matrix, (b) permuted matrix, (c) partitioned matrix (eight substructures and the interface boundary are defined).

$$\begin{bmatrix} \mathbf{K}_s & \mathbf{K}_c \\ \mathbf{K}_c^T & \mathbf{K}_b \end{bmatrix} \begin{bmatrix} \mathbf{u}_s \\ \mathbf{u}_b \end{bmatrix} = \lambda \begin{bmatrix} \mathbf{M}_s & \mathbf{M}_c \\ \mathbf{M}_c^T & \mathbf{M}_b \end{bmatrix} \begin{bmatrix} \mathbf{u}_s \\ \mathbf{u}_b \end{bmatrix}, \tag{18}$$

where the subscripts s and b present the substructural and interface boundary terms, respectively, and the subscript c presents the coupled terms between s and b.

In Eq. (18), the component matrices $\mathbf{M}_s$, $\mathbf{K}_s$, $\mathbf{M}_c$, and $\mathbf{K}_c$ are represented in a submatrix form as

$$\mathbf{M}_s = \begin{bmatrix} \mathbf{M}_1^s & & \mathbf{0} \\ & \ddots & \\ \mathbf{0} & & \mathbf{M}_n^s \end{bmatrix}, \mathbf{K}_s = \begin{bmatrix} \mathbf{K}_1^s & & \mathbf{0} \\ & \ddots & \\ \mathbf{0} & & \mathbf{K}_n^s \end{bmatrix}, \mathbf{M}_c = \begin{bmatrix} \mathbf{M}_1^c \\ \vdots \\ \mathbf{M}_n^c \end{bmatrix}, \mathbf{K}_c = \begin{bmatrix} \mathbf{K}_1^c \\ \vdots \\ \mathbf{K}_n^c \end{bmatrix}, \tag{19}$$

where $\mathbf{M}_i^s$ and $\mathbf{K}_i^s$ are the substructural mass and stiffness matrices corresponding to the i^{th} substructure, respectively. $\mathbf{M}_i^c$ and $\mathbf{K}_i^c$ are the coupled mass and stiffness matrices between the i^{th} substructure and the interface boundary, respectively.

3.2. Substructural stiffness condensation

Expanding the first row in Eq. (18), the substructural displacement vector $\mathbf{u}_s$ is expressed by

$$\begin{aligned} \mathbf{u}_s &= -(\mathbf{K}_s - \lambda \mathbf{M}_s)^{-1}(\mathbf{K}_c - \lambda \mathbf{M}_c)\mathbf{u}_b \\ &= [-\mathbf{K}_s^{-1}\mathbf{K}_c + \lambda \mathbf{K}_s^{-1}(\mathbf{M}_c + \mathbf{M}_s \boldsymbol{\Psi}_c) + o(\lambda^2) + o(\lambda^3) + \cdots]\mathbf{u}_b, \end{aligned} \tag{20}$$

and neglecting the terms with the unknown global eigenvalue λ, the substructural displacement vector $\mathbf{u}_s$ can be approximated by the interface displacement vector $\mathbf{u}_b$

$$\mathbf{u}_s \approx \bar{\mathbf{u}}_s = \boldsymbol{\Psi}_c \mathbf{u}_b \ \text{ with } \boldsymbol{\Psi}_c = -\mathbf{K}_s^{-1}\mathbf{K}_c, \tag{21}$$

where $\boldsymbol{\Psi}_c$ denotes the constraint mode matrix [30] to couple the substructures with the interface boundary.

Then, the global displacement vector $\mathbf{u}_g$ is approximated by using $\bar{\mathbf{u}}_s$ in Eq. (21)

$$\mathbf{u}_g \approx \bar{\mathbf{u}}_g = \begin{bmatrix} \bar{\mathbf{u}}_s \\ \mathbf{u}_b \end{bmatrix} = \boldsymbol{\Psi}\mathbf{u}_b \ \text{ with } \boldsymbol{\Psi} = \begin{bmatrix} \boldsymbol{\Psi}_c \\ \mathbf{I}_b \end{bmatrix}, \tag{22}$$

in which $\boldsymbol{\Psi}$ is the interface constraint mode matrix [30], and is represented in a submatrix form as

$$\boldsymbol{\Psi} = \begin{bmatrix} \boldsymbol{\Psi}_1^c \\ \vdots \\ \boldsymbol{\Psi}_n^c \\ \mathbf{I}_b \end{bmatrix} \text{ with } \boldsymbol{\Psi}_i^c = -(\mathbf{K}_i^s)^{-1}\mathbf{K}_i^c \ \text{ for } i = 1, 2, \cdots, n, \tag{23}$$

where $\boldsymbol{\Psi}_i^c$ denotes the constraint mode matrix to couple the i^{th} substructure with the interface boundary, and $\mathbf{I}_b$ denotes the identity matrix for the interface boundary.

Conducting the Rayleigh-Ritz analysis with $\boldsymbol{\Psi}$ in Eq. (22), the following reduced eigenvalue problem is given by

$$\hat{\mathbf{K}}_b \mathbf{u}_b = \hat{\lambda} \hat{\mathbf{M}}_b \mathbf{u}_b \ \text{ with } \hat{\mathbf{M}}_b = \boldsymbol{\Psi}^T \mathbf{M}_g \boldsymbol{\Psi}, \hat{\mathbf{K}}_b = \boldsymbol{\Psi}^T \mathbf{K}_g \boldsymbol{\Psi}, \tag{24}$$

in which $\hat{\mathbf{M}}_b$ and $\hat{\mathbf{K}}_b$ are the reduced mass and stiffness matrices, and those are $N_b \times N_b$ matrices (N_b is the number of DOFs in the interface boundary). Here, $\hat{\lambda}$ is the approximated eigenvalue of the reduced system, which is constructed using the substructural stiffness condensation.

In addition, using Eqs. (19) and (23), the reduced matrices $\hat{\mathbf{M}}_b$ and $\hat{\mathbf{K}}_b$ in Eq. (24) can be effectively calculated at the submatrix level through the following submatrix operations

$$\hat{\mathbf{M}}_b = \mathbf{M}_b + \sum_{i=1}^{n} (\mathbf{M}_i^c)^T \boldsymbol{\Psi}_i^c + \sum_{i=1}^{n} (\boldsymbol{\Psi}_i^c)^T \hat{\mathbf{M}}_i^c \text{ with } \hat{\mathbf{M}}_i^c = \mathbf{M}_i^c + \mathbf{M}_i \boldsymbol{\Psi}_i^c, \tag{25a}$$

$$\hat{\mathbf{K}}_b = \mathbf{K}_b + \sum_{i=1}^{n} (\mathbf{K}_i^c)^T \boldsymbol{\Psi}_i^c. \tag{25b}$$

3.3. Interface boundary reduction

After solving the reduced eigenvalue problem in Eq. (24), the interface eigenvector matrix $\boldsymbol{\Phi}_b$ is calculated, and the interface displacement vector $\mathbf{u}_b$ is expressed as

$$\mathbf{u}_b = \boldsymbol{\Phi}_b \mathbf{q}_b = [\boldsymbol{\Phi}_b^d \ \ \boldsymbol{\Phi}_b^r] \begin{bmatrix} \mathbf{q}_b^d \\ \mathbf{q}_b^r \end{bmatrix}, \tag{26}$$

where $\boldsymbol{\Phi}_b$ is decomposed into $\boldsymbol{\Phi}_b^d$ and $\boldsymbol{\Phi}_b^r$, the eigenvector matrices corresponding to the dominant and residual interface normal modes, respectively, and $\mathbf{q}_b^d$ and $\mathbf{q}_b^r$ are their generalized coordinate vectors.

Considering only the dominant terms $\boldsymbol{\Phi}_b^d$ and $\mathbf{q}_b^d$, the reduced interface displacement vector $\bar{\mathbf{u}}_b$ is obtained as

$$\mathbf{u}_b \approx \bar{\mathbf{u}}_b = \boldsymbol{\Phi}_b^d \mathbf{q}_b^d. \tag{27}$$

Applying Eq. (27) into Eq. (24) and pre-multiplying $(\boldsymbol{\Phi}_b^d)^T$, the eigenvalue problem for the reduced interface boundary is given by

$$\bar{\mathbf{K}}_\mathbf{b} \mathbf{q}_\mathbf{b}^\mathbf{d} = \bar{\lambda} \bar{\mathbf{M}}_\mathbf{b} \mathbf{q}_\mathbf{b}^\mathbf{d} \quad \textbf{with } \bar{\mathbf{M}}_\mathbf{b} = (\boldsymbol{\Phi}_\mathbf{b}^\mathbf{d})^\mathbf{T} \hat{\mathbf{M}}_\mathbf{b} (\boldsymbol{\Phi}_\mathbf{b}^\mathbf{d}), \bar{\mathbf{K}}_\mathbf{b} = (\boldsymbol{\Phi}_\mathbf{b}^\mathbf{d})^\mathbf{T} \hat{\mathbf{K}}_\mathbf{b} (\boldsymbol{\Phi}_\mathbf{b}^\mathbf{d}), \tag{28}$$

in which $\bar{\mathbf{M}}_b$ and $\bar{\mathbf{K}}_b$ denote the mass and stiffness matrices for the reduced interface boundary, respectively, and $\bar{\lambda}$ is the approximated eigenvalue obtained from the above eigenvalue problem. Herein, $\bar{\mathbf{M}}_b$ and $\bar{\mathbf{K}}_b$ are $\bar{N}_b \times \bar{N}_b$ matrices, where $\bar{N}_b$ is the number of the dominant interface normal modes selected.

3.4. Iterative substructural inertial effect condensation

In Eq. (20), considering the first order term of λ, the approximated substructural displacement vector $\bar{\mathbf{u}}_s$ in Eq. (21) can be expressed more precisely

$$\bar{\mathbf{u}}_s = \boldsymbol{\Psi}_c \mathbf{u}_b + \lambda \mathbf{K}_s^{-1}(\mathbf{M}_c \mathbf{u}_b + \mathbf{M}_s \boldsymbol{\Psi}_c \mathbf{u}_b). \tag{29}$$

From the relation $\bar{\mathbf{u}}_s = \boldsymbol{\Psi}_c \mathbf{u}_b$ in Eq. (21), the term $\boldsymbol{\Psi}_c \mathbf{u}_b$ in the right-hand side of Eq. (29) can be replaced with $\bar{\mathbf{u}}_s$ as follow

$$\bar{\mathbf{u}}_s = \boldsymbol{\Psi}_c \mathbf{u}_b + \lambda \mathbf{K}_s^{-1}(\mathbf{M}_c \mathbf{u}_b + \mathbf{M}_s \bar{\mathbf{u}}_s). \tag{30}$$

Using $\bar{\mathbf{u}}_b$ ($= \boldsymbol{\Phi}_b^d \mathbf{q}_b^d$) in Eq. (27) instead of $\mathbf{u}_b$, and using $\bar{\lambda}$ instead of λ, the following equation is obtained

$$\bar{\mathbf{u}}_s = \bar{\boldsymbol{\Psi}}_c \mathbf{q}_b^d + \bar{\lambda} \mathbf{K}_s^{-1}(\bar{\mathbf{M}}_\mathbf{c} \mathbf{q}_\mathbf{b}^\mathbf{d} + \mathbf{M}_s \bar{\mathbf{u}}_\mathbf{s}) \quad \text{with } \bar{\boldsymbol{\Psi}}_\mathbf{c} = \boldsymbol{\Psi}_\mathbf{c} \boldsymbol{\Phi}_\mathbf{b}^\mathbf{d}, \bar{\mathbf{M}}_\mathbf{c} = \mathbf{M}_\mathbf{c} \boldsymbol{\Phi}_\mathbf{b}^\mathbf{d}. \tag{31}$$

Let us assume a transformation matrix $\boldsymbol{\Theta}$ between $\bar{\mathbf{u}}_s$ and $\mathbf{q}_b^d$. The approximated substructural displacement vector $\bar{\mathbf{u}}_s$ can be represented by

$$\bar{\mathbf{u}}_s = \boldsymbol{\Theta} \mathbf{q}_b^d. \tag{32}$$

Thus, $\bar{\mathbf{u}}_s$ in the right-hand side of Eq. (31) can be replaced with $\boldsymbol{\Theta}\mathbf{q}_b^d$ as follows

$$\bar{\mathbf{u}}_s = [\bar{\boldsymbol{\Psi}}_c + \bar{\lambda} \mathbf{K}_s^{-1}(\bar{\mathbf{M}}_c + \mathbf{M}_s \boldsymbol{\Theta})] \mathbf{q}_b^d. \tag{33}$$

From Eqs. (32) and (33), the transformation matrix $\boldsymbol{\Theta}$ can be defined by

$$\boldsymbol{\Theta} = \bar{\boldsymbol{\Psi}}_c + \bar{\lambda} \mathbf{K}_s^{-1}(\bar{\mathbf{M}}_c + \mathbf{M}_s \boldsymbol{\Theta}). \tag{34}$$

Using Eqs. (27), (32) and (34), the approximated global displacement vector $\bar{\mathbf{u}}_g$ in Eq. (22) is redefined as

$$\bar{\mathbf{u}}_g = \begin{bmatrix} \bar{\mathbf{u}}_s \\ \bar{\mathbf{u}}_b \end{bmatrix} = \mathbf{T}\mathbf{q}_b^d, \tag{35a}$$

$$\text{with } \mathbf{T} = \begin{bmatrix} \boldsymbol{\Theta} \\ \boldsymbol{\Phi}_b^d \end{bmatrix} = \bar{\boldsymbol{\Psi}} + \bar{\lambda}\boldsymbol{\Psi}_a, \bar{\boldsymbol{\Psi}} = \begin{bmatrix} \bar{\boldsymbol{\Psi}}_c \\ \boldsymbol{\Phi}_b^d \end{bmatrix}, \boldsymbol{\Psi}_a = \begin{bmatrix} \mathbf{K}_s^{-1}(\bar{\mathbf{M}}_c + \mathbf{M}_s\boldsymbol{\Theta}) \\ \mathbf{0} \end{bmatrix}, \tag{35b}$$

where $\mathbf{T}$ is a newly defined interface constraint mode matrix compensating the substructural inertial effects by $\bar{\lambda}\boldsymbol{\Psi}_a$, and $\bar{\boldsymbol{\Psi}}$ is the reduced interface constraint mode matrix.

Pre-multiplying $\bar{\mathbf{M}}_b^{-1}$ in Eq. (28), we obtain the following relation

$$\bar{\lambda}\mathbf{q}_b^d = \mathbf{H}_b\mathbf{q}_b^d \text{ with } \mathbf{H}_b = \bar{\mathbf{M}}_b^{-1}\bar{\mathbf{K}}_b, \tag{36}$$

and using this relationship, the transformation matrix $\boldsymbol{\Theta}$ in Eq. (34) can be rewritten as

$$\boldsymbol{\Theta} = \bar{\boldsymbol{\Psi}}_c + \mathbf{K}_s^{-1}(\bar{\mathbf{M}}_c + \mathbf{M}_s\boldsymbol{\Theta})\mathbf{H}_b, \tag{37}$$

in which the transformation matrix $\boldsymbol{\Theta}$ cannot be directly calculated due to its implicit form, and thus it should be calculated using an iterative procedure.

Employing the iterative scheme of the IIRS method [7], the iterative transformation matrix $\boldsymbol{\Theta}^{(k)}$ can be defined as

$$\boldsymbol{\Theta}^{(k)} = \bar{\boldsymbol{\Psi}}_c + \mathbf{K}_s^{-1}(\bar{\mathbf{M}}_c + \mathbf{M}_s\boldsymbol{\Theta}^{(k-1)})\mathbf{H}_b^{(k-1)} \text{ for } k \geqslant 2, \boldsymbol{\Theta}^{(1)} = \bar{\boldsymbol{\Psi}}_c, \mathbf{H}_b^{(1)} = \mathbf{H}_b, \tag{38}$$

where superscript k denotes the k^{th} iteration. Therefore, the iterative transformation matrix $\mathbf{T}^{(k)}$ can be defined as

$$\mathbf{T}^{(k)} = \begin{bmatrix} \boldsymbol{\Theta}^{(k)} \\ \boldsymbol{\Phi}_b^d \end{bmatrix} = \bar{\boldsymbol{\Psi}} + \mathbf{E}^{(k-1)} \quad \text{for } k \geqslant 2, \tag{39}$$

in which

$$\mathbf{E}^{(k-1)} = \begin{bmatrix} \mathbf{B}^{(k-1)} \\ \mathbf{0} \end{bmatrix} \text{ with } \mathbf{B}^{(k-1)} = \mathbf{K}_s^{-1}(\bar{\mathbf{M}}_c + \mathbf{M}_s\boldsymbol{\Theta}^{(k-1)})\mathbf{H}_b^{(k-1)}, \tag{40a}$$

$$\mathbf{T}^{(1)} = \bar{\boldsymbol{\Psi}}. \tag{40b}$$

Note that, when $k = 2$, $\mathbf{T}^{(k)}$ is equivalent to the transformation matrix of the algebraic dynamic condensation method [1].

Finally, the reduced mass and stiffness matrices for the k^{th} iteration are obtained by

$$\tilde{\mathbf{M}}_b^{(k)} = (\mathbf{T}^{(k)})^T\mathbf{M}_g\mathbf{T}^{(k)} = \bar{\mathbf{M}}_b + \bar{\boldsymbol{\Psi}}^T\mathbf{M}_g\mathbf{E}^{(k-1)} + (\mathbf{E}^{(k-1)})^T\mathbf{M}_g\bar{\boldsymbol{\Psi}} + (\mathbf{E}^{(k-1)})^T\mathbf{M}_g\mathbf{E}^{(k-1)}, \tag{41a}$$

$$\tilde{\mathbf{K}}_b^{(k)} = (\mathbf{T}^{(k)})^T\mathbf{K}_g\mathbf{T}^{(k)} = \bar{\mathbf{K}}_b + \bar{\boldsymbol{\Psi}}^T\mathbf{K}_g\mathbf{E}^{(k-1)} + (\mathbf{E}^{(k-1)})^T\mathbf{K}_g\bar{\boldsymbol{\Psi}} + (\mathbf{E}^{(k-1)})^T\mathbf{K}_g\mathbf{E}^{(k-1)}, \tag{41b}$$

in which

$$\bar{\boldsymbol{\Psi}}^T\mathbf{M}_g\mathbf{E}^{(k-1)} = (\boldsymbol{\Phi}_b^d)^T\hat{\mathbf{M}}_c^T\mathbf{B}^{(k-1)}, (\mathbf{E}^{(k-1)})^T\mathbf{M}_g\mathbf{E}^{(k-1)} = (\mathbf{B}^{(k-1)})^T\mathbf{M}_s\mathbf{B}^{(k-1)}, \tag{42a}$$

$$\bar{\boldsymbol{\Psi}}^T\mathbf{K}_g\mathbf{E}^{(k-1)} = \mathbf{0}, (\mathbf{E}^{(k-1)})^T\mathbf{K}_g\mathbf{E}^{(k-1)} = (\mathbf{B}^{(k-1)})^T\mathbf{K}_s\mathbf{B}^{(k-1)}, \tag{42b}$$

$$\tilde{\mathbf{M}}_b^{(1)} = \bar{\mathbf{M}}_b, \tilde{\mathbf{K}}_b^{(1)} = \bar{\mathbf{K}}_b, \tag{42c}$$

in which $\tilde{\mathbf{M}}_b^{(1)}$ and $\tilde{\mathbf{K}}_b^{(1)}$ are the initial reduced mass and stiffness matrices.

In Eq. (38), the matrix $\mathbf{H}_b^{(k-1)}$ in $\boldsymbol{\Theta}^{(k)}$ is calculated using the following equation

$$\mathbf{H}_b^{(k-1)} = (\tilde{\mathbf{M}}_b^{(k-1)})^{-1}\tilde{\mathbf{K}}_b^{(k-1)} \quad \text{for } k \geqslant 2, \tag{43}$$

where $\tilde{\mathbf{M}}_b^{(k-1)}$ and $\tilde{\mathbf{K}}_b^{(k-1)}$ are the reduced mass and stiffness matrices for the $(k-1)^{\text{th}}$ iteration, respectively.

The matrices $\hat{\mathbf{M}}_c$ and $\mathbf{B}^{(k-1)}$ in Eq. (42) are represented in a submatrix form as

$$\hat{\mathbf{M}}_c = \begin{bmatrix} \hat{\mathbf{M}}_1^c \\ \hat{\mathbf{M}}_2^c \\ \vdots \\ \hat{\mathbf{M}}_n^c \end{bmatrix}, \mathbf{B}^{(k-1)} = \begin{bmatrix} \mathbf{B}_1^{(k-1)} \\ \mathbf{B}_2^{(k-1)} \\ \vdots \\ \mathbf{B}_n^{(k-1)} \end{bmatrix} \text{ with } \mathbf{B}_i^{(k-1)} = (\mathbf{K}_i^s)^{-1}(\mathbf{M}_i^c + \mathbf{M}_i\boldsymbol{\Theta}_i^{(k-1)})\mathbf{H}_b^{(k-1)}. \tag{44}$$

Using the submatrix forms of $\mathbf{M}_s$ and $\mathbf{K}_s$ in Eq. (19), and $\hat{\mathbf{M}}_c$ and $\mathbf{B}^{(k-1)}$ in Eq. (44), the iterative reduced matrices of the proposed method are finally obtained in a submatrix form as follows:

$$\tilde{\mathbf{M}}_b^{(k)} = \bar{\mathbf{M}}_b + \mathbf{R}_1 + \mathbf{R}_1^T + \mathbf{R}_2, \tilde{\mathbf{K}}_b^{(k)} = \bar{\mathbf{K}}_b + \mathbf{R}_3, \tag{45}$$

with

$$\mathbf{R}_1 = \sum_{i=1}^{n}(\boldsymbol{\Phi}_b^d)^T(\hat{\mathbf{M}}_i^c)^T\mathbf{B}_i^{(k-1)}, \mathbf{R}_2 = \sum_{i=1}^{n}(\mathbf{B}_i^{(k-1)})^T\mathbf{M}_i^s\mathbf{B}_i^{(k-1)}, \mathbf{R}_3 = \sum_{i=1}^{n}(\mathbf{B}_i^{(k-1)})^T\mathbf{K}_i^s\mathbf{B}_i^{(k-1)}, \tag{46}$$

in which $\tilde{\mathbf{M}}_b^{(k)}$ and $\tilde{\mathbf{K}}_b^{(k)}$ are $\bar{N}_b \times \bar{N}_b$ matrices.

The strength of the proposed method is that, the iterative reduced matrices are efficiently calculated through simple multiplications and summations of very small submatrices without considering the global transformation matrix, which may incur huge computational cost due to the iterative updated procedure of large matrices. In addition, the computer memory utilized during the iterative procedure can be reduced, thanks to the compact formulation developed.

Then, the approximated eigensolutions are calculated from the following reduced eigenvalue problem

$$\tilde{\mathbf{K}}_b^{(k)}(\bar{\boldsymbol{\varphi}})_i = \bar{\lambda}_i\tilde{\mathbf{M}}_b^{(k)}(\bar{\boldsymbol{\varphi}})_i \quad \text{for } i = 1, 2, \cdots, \bar{N}_b, \tag{47}$$

where $\bar{\lambda}_i$ and $(\bar{\boldsymbol{\varphi}})_i$ are the approximated eigenvalues and eigenvectors, respectively.

The approximated global eigenvectors are calculated by

$$(\bar{\boldsymbol{\varphi}}_g)_i = \mathbf{T}^{(k)}\bar{\boldsymbol{\varphi}}_i \quad \text{for } i = 1, 2, \cdots, \bar{N}_b, \tag{48}$$

in which

$$\mathbf{T}^{(k)} = \begin{bmatrix} \mathbf{T}_1^{(k)} \\ \mathbf{T}_2^{(k)} \\ \vdots \\ \mathbf{T}_n^{(k)} \\ \boldsymbol{\Phi}_b^d \end{bmatrix} \text{ with } \mathbf{T}_i^{(k)} = \boldsymbol{\Psi}_i^c\boldsymbol{\Phi}_b^d + \mathbf{B}_i^{(k-1)} \text{ for } i = 1, 2, \cdots, n. \tag{49}$$

The computational procedure of the iterative algebraic dynamic condensation is described in Fig. 2.

4. Numerical examples

To demonstrate the performance of the proposed method, we conduct numerical tests with practical structural FE models: a rectangular plate, a stiffened plate, a semi-submersible rig, and a barge ship. The numerical results are compared to those of the IIRS method, and to verify the accuracy of the reduced models obtained

using the proposed and IIRS methods, the following relative eigenvalue error is employed

$$\xi_i = \frac{\bar{\lambda}_i - \lambda_i}{\lambda_i}, \tag{50}$$

in which ξ_i and λ_i denote the relative eigenvalue error for the i^{th} mode and the exact global eigenvalue, that are obtained from the original FE model, respectively, and $\bar{\lambda}_i$ denotes the approximated eigenvalue for the i^{th} mode obtained from the reduced eigenvalue problem in Eq. (47).

The MITC shell finite elements [44–46] are used for the FE modeling. A free boundary condition is applied to all FE models, and we use the material property of a typical mild steel, with Young's modulus E = 206 GPa, Poisson's ratio $\upsilon = 0.3$, and density $\rho = 7,850\ \text{kg/m}^3$. MATLAB is used for implementation of the numerical procedures, and a personal computer (Intel core (TM) i7-3770, 3.40 GHz CPU, and 32 GB RAM) is used for computation.

In the IIRS method, the retained DOFs are selected considering the ratio of the diagonal entries of mass and stiffness matrices [10]. In the proposed method, METIS [47], an efficient matrix reordering and partitioning software package, is used for algebraic substructuring, and to select the dominant interface normal modes [30], we use the frequency cut-off technique [30]. We assign the error tolerance 10^{-4} as a strict criterion to ensure the accuracy of the reduced models in the engineering perspective, and observe the iteration counts to satisfy the assigned error tolerance.

4.1. Rectangular plate problem

As shown in Fig. 3, a rectangular plate is modeled using a 60×36 mesh (11,285 DOFs). For the IIRS and proposed methods, we consider reduced models of the same size, $N_r = 100$ and $\bar{N}_b = 100$. For the proposed method, the global matrices are partitioned into 16 substructures and the interface boundary using algebraic substructuring. We investigate the iteration counts of both methods, until the relative eigenvalue errors corresponding to 1^{st}–20^{th} modes satisfy the error tolerance.

Fig. 4 shows the relative eigenvalue errors obtained by the IIRS and proposed methods. The IIRS method cannot give solutions satisfying the error tolerance even by the 10^{th} iteration. However,

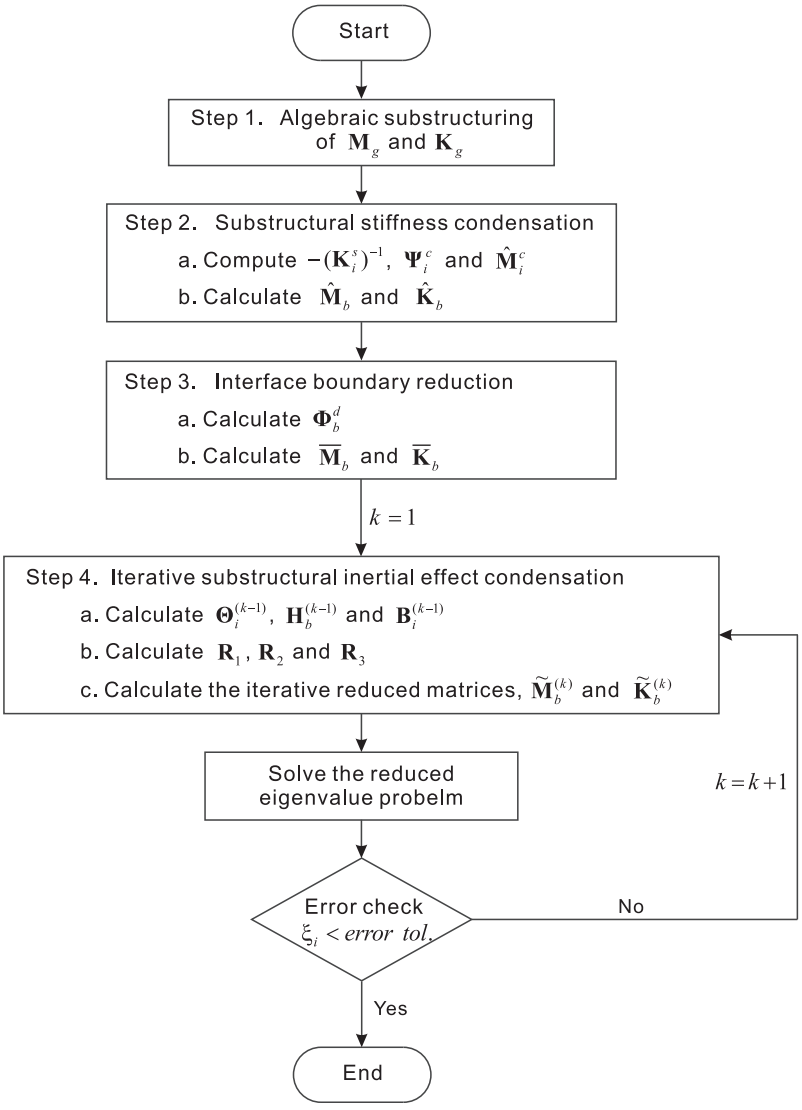

Fig. 2. Computational procedure of the iterative algebraic dynamic condensation method.

with the proposed method, the desired solutions are obtained by the 5th iteration. Table 1 and Table 2 show the relative eigenvalue errors and the specific computational costs; when the iteration counts for the IIRS and proposed methods are 10 and 5, respectively. The numerical results show that the proposed method constructs more accurate reduced models than the IIRS method, with much less computational cost. Therefore, we can easily identify that the proposed method is superior to the IIRS method regarding solution accuracy and computational efficiency.

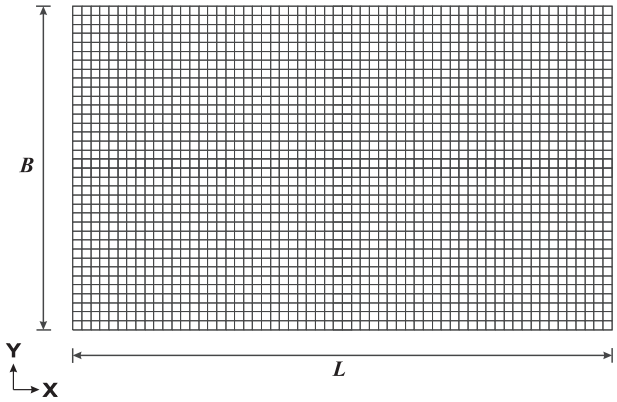

Fig. 3. Rectangular plate problem (60×36 mesh, 11,285 DOFs, length $L = 20$ m, width $B = 12$ m, thickness $t = 0.025$ m).

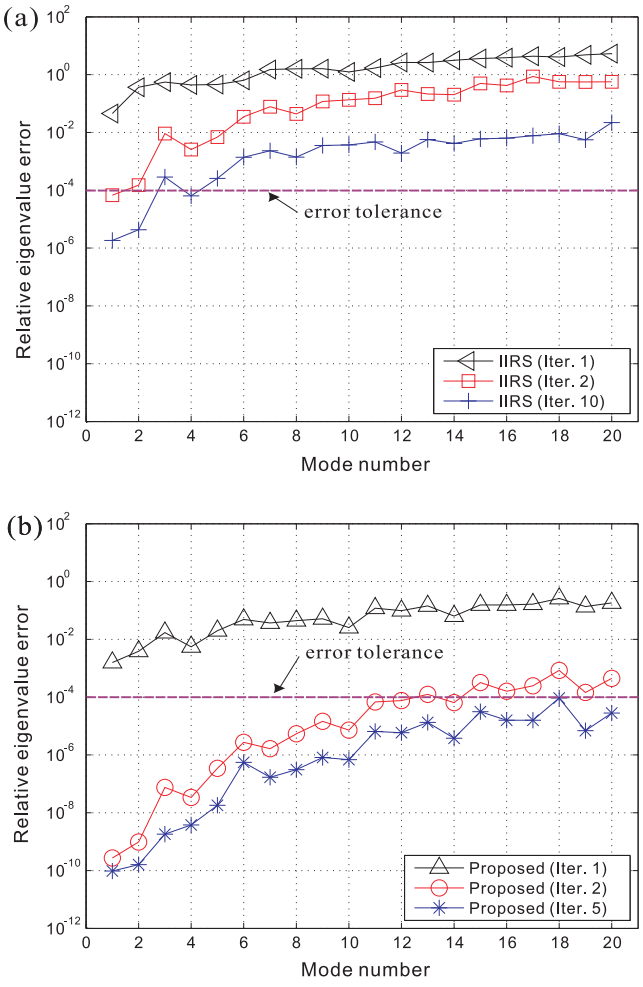

Fig. 4. Relative eigenvalue errors for the rectangular plate problem, when $N_r = \bar{N}_b = 100$: (a) 1st, 2nd, and 10th iterations by the IIRS method, (b) 1st, 2nd, and 5th iterations by the proposed method.

Table 1
Relative eigenvalue errors for the rectangular plate problem in Fig. 4.

Mode number	IIRS 10th iteration	Proposed 5th iteration
1	1.83717E−06	9.26733E−11
2	4.29073E−06	2.55235E−10
3	2.85734E−04	1.49123E−09
4	6.41667E−05	4.26750E−09
5	2.58734E−04	1.83683E−08
6	1.38521E−03	5.57216E−07
7	2.33068E−03	1.68671E−07
8	1.39510E−03	3.08088E−07
9	3.53615E−03	8.13839E−07
10	3.71868E−03	6.91319E−07
11	4.67691E−03	6.49403E−06
12	1.94286E−03	5.87819E−06
13	5.67465E−03	1.34455E−05
14	4.18013E−03	3.80472E−06
15	6.02451E−03	3.14492E−05
16	6.35450E−03	1.59214E−05
17	7.74027E−03	1.59703E−05
18	9.08663E−03	9.30836E−05
19	5.56733E−03	6.95991E−06
20	2.19049E−02	2.82683E−05

Table 2
Specific computational costs for the rectangular plate problem, corresponding to 10th iteration by the IIRS method and 5th iteration by the proposed method.

Methods	Items	Computation times	
		[sec]	Ratio [%]
IIRS	Transformation procedure	195.94	71.47
	Iterative transformation procedure	78.09	28.48
	Reduced eigenvalue problem	0.12	0.05
	Total	274.15	100.00
Proposed	Algebraic substructuring	0.05	0.02
	Substructural stiffness condensation	0.63	0.23
	Interface boundary reduction	0.48	0.18
	Substructural inertial effect condensation	0.25	0.09
	Iterative transformation procedure	3.56	1.30
	Reduced eigenvalue problem	0.12	0.04
	Total	5.09	1.86

We also investigate the convergence characteristic of the proposed method compared to the IIRS method. Fig. 5 shows the convergence of relative eigenvalue errors corresponding to the 9th and 10th modes with respect to the iteration counts. The relative eigenvalue errors at each iteration are listed in Table 3. In Fig. 5, the solutions obtained by the IIRS method converge slowly with each iteration, and the solutions are saturated at the relative eigenvalue error of 10^{-3}. On the other hand, the solutions obtained by the proposed method converge very quickly at the 2nd iteration. After that, the solution accuracies are saturated near the relative eigenvalue error of 10^{-7}. We can identify that the convergence of the proposed method is faster than that of the IIRS method. Note that, as the size of the reduced models increases, the saturation happens at more accurate solutions in both methods.

4.2. Stiffened plate problem

A stiffened plate, which has 8,580 shell finite elements and 52,662 DOFs, is considered as shown in Fig. 6. We consider reduced models of the same size, $N_r = 300$ and $\bar{N}_b = 300$, for both methods.

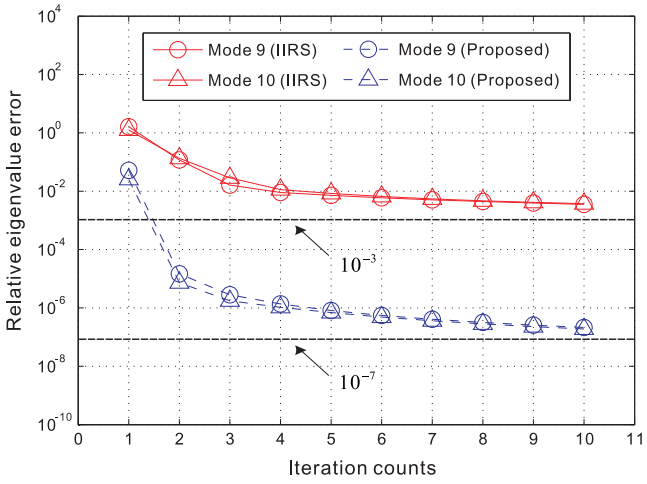

Fig. 5. Convergence of the relative eigenvalue errors corresponding to 9th and 10th modes for the rectangular plate problem.

The global mass and stiffness matrices are partitioned into 64 substructures using the proposed method. The iteration procedure is conducted until the relative eigenvalue errors corresponding to 1st–50th modes satisfy the error tolerance.

Fig. 7 presents the relative eigenvalue errors obtained using the IIRS and proposed methods. The values of the relative eigenvalue errors corresponding to the 31th–50th global modes are listed in Table 4, and the specific computational costs are described in Table 5, when the iteration counts for the IIRS and proposed methods are 10 and 4. It is observed that the proposed method can provide reduced models satisfying the error tolerance with fewer iterations and at less computational cost than with the IIRS method.

4.3. Semi-submersible rig problem

Let us consider a semi-submersible rig structure using 16,800 shell finite elements as shown in Fig. 8. The total number of DOFs is 102,054. The iteration procedure is stopped when the relative eigenvalue errors corresponding to 1st–70th modes are within the error tolerance designated.

Unfortunately, with the IIRS method, the matrix $\mathbf{T}_1^{(k)}$ in Eq. (14) is an almost fully populated matrix and requires a great deal of computer memory. For this reason, we fail to obtain reduced models of any size. Using the proposed method, the global mass and stiffness matrices are partitioned into 128 substructures, and two numerical cases, $\bar{N}_b = 350$ and $\bar{N}_b = 600$, are considered, as shown in Fig. 9. For the first numerical case, the reduced model satisfying the error tolerance is obtained at the 5th iteration, and for the sec-

Table 3
Relative eigenvalue errors corresponding to 9th and 10th modes with respect to the iteration counts for the rectangular plate problem.

Iteration counts	IIRS Mode No.		Proposed Mode No.	
	9	10	9	10
1	1.61947E+00	1.24922E+00	5.17449E−02	2.56102E−02
2	1.18145E−01	1.34452E−01	1.46515E−05	7.25138E−06
3	1.62017E−02	2.86258E−02	2.82130E−06	1.74850E−06
4	9.02742E−03	1.13916E−02	1.36496E−06	1.04684E−06
5	7.17427E−03	8.36240E−03	8.13464E−07	6.91348E−07
6	5.94566E−03	6.58967E−03	5.53511E−07	4.88093E−07
7	5.07348E−03	5.45980E−03	4.08237E−07	3.63435E−07
8	4.42352E−03	4.69048E−03	3.18380E−07	2.82000E−07
9	3.92458E−03	4.13548E−03	2.57491E−07	2.27717E−07
10	3.53612E−03	3.71872E−03	2.13464E−07	1.89763E−07

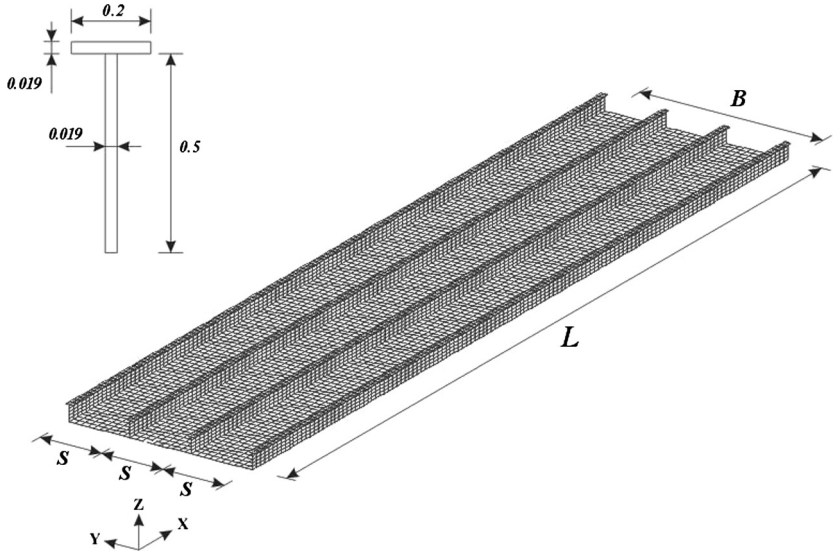

Fig. 6. Stiffened plate problem (8,580 shell elements, 52,662 DOFs, length $L = 26$ m, breadth $B = 6$ m, stiffener spacing $S = 2$ m, thickness $t = 0.019$ m).

ond numerical case, the tolerance is satisfied at the 3rd iteration. Table 6 shows the computational costs, when $\bar{N}_b = 350$. The IIRS method is unable to solve large FE models, but the proposed method provides reduced models with relatively accurate solutions and lower computational cost.

4.4. Barge ship problem

Finally, we consider a barge ship, as shown in Fig. 10. The FE model is constructed with 26,688 shell finite elements and 26,228 nodes, and the number of DOFs is 157,368. In this problem, the IIRS method also does not work. The error tolerance is given for the relative eigenvalue errors corresponding to the 1st–50th modes.

To construct the reduced model, the global mass and stiffness matrices are partitioned into 128 substructures, and two numerical cases are considered: $\bar{N}_b = 300$ and $\bar{N}_b = 500$. For the two cases considered, we obtain the desired reduced models after the 5th and 4th iterations, respectively, as shown in Fig. 11. Table 7 presents the computational cost when $\bar{N}_b = 300$. The results show that the proposed method can handle large FE models with excellent solution accuracy and computational efficiency, compared to the IIRS method.

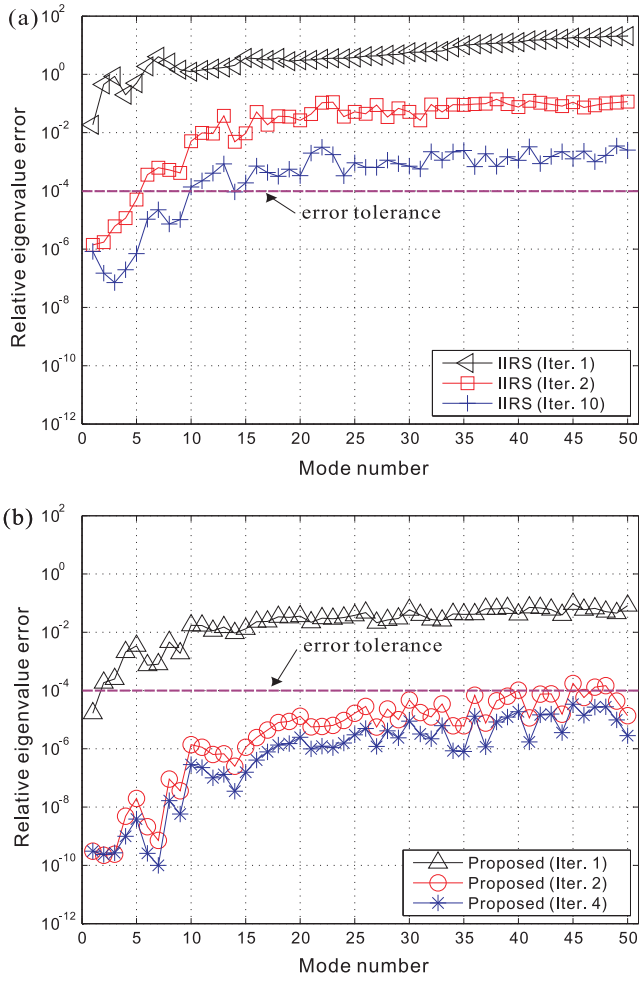

Fig. 7. Relative eigenvalue errors for the stiffened plate problem, when $N_r = \bar{N}_b = 300$: (a) 1st, 2nd, and 10th iterations by the IIRS method, (b) 1st, 2nd, and 4th iterations by the proposed method.

Table 4
Relative eigenvalue errors corresponding to the 31th–50th global modes for the stiffened structure problem in Fig. 7.

Mode number	IIRS 10th iteration	Proposed 4th iteration
31	5.63361E−04	3.21188E−06
32	2.20046E−03	2.21368E−06
33	1.13481E−03	6.24921E−06
34	2.17261E−03	8.51955E−07
35	2.43465E−03	8.12732E−07
36	6.77522E−04	1.30282E−05
37	1.87634E−03	1.17182E−06
38	6.91542E−04	8.34432E−06
39	1.47968E−03	1.22617E−05
40	1.11207E−03	1.86428E−05
41	3.25655E−03	1.72035E−06
42	8.58681E−04	1.45410E−05
43	1.51598E−03	1.56174E−05
44	2.20489E−03	3.58203E−06
45	1.26197E−03	3.39884E−05
46	2.31364E−03	1.41170E−05
47	9.98438E−04	2.70284E−05
48	1.65159E−03	2.74856E−05
49	3.46007E−03	9.76741E−06
50	2.51780E−03	2.82249E−06

Table 5
Specific computational costs for the stiffened structure problem, corresponding to the 10th iteration by the IIRS method and 4th iteration by the proposed method.

Methods	Items	Computation times	
		[sec]	Ratio [%]
IIRS	Transformation procedure	3813.72	62.84
	Iterative transformation procedure	2254.95	37.15
	Reduced eigenvalue problem	0.62	0.01
	Total	6069.29	100.00
Proposed	Algebraic substructuring	0.52	0.01
	Substructural stiffness condensation	11.07	0.18
	Interface boundary reduction	17.3	0.29
	Substructural inertial effect condensation	5.56	0.09
	Iterative transformation procedure	54.02	0.89
	Reduced eigenvalue problem	0.62	0.01
	Total	89.09	1.47

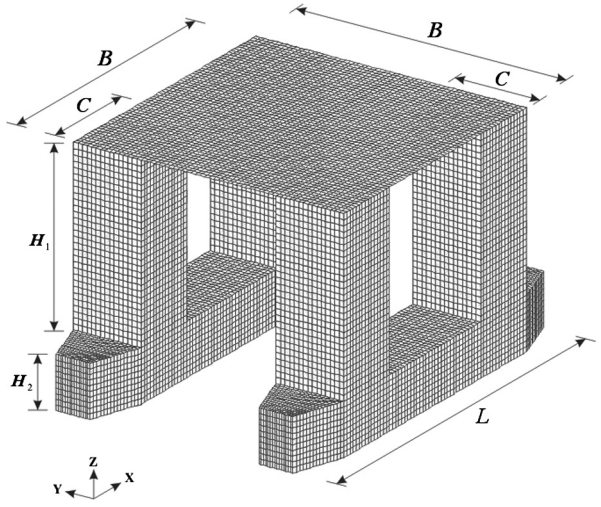

Fig. 8. Semi-submersible rig problem (16,800 shell elements, 102,054 DOFs, length $L = 110$ m, breadth $B = 80$ m, column width $C = 20$ m, height $H_1 = 50$ m, height $H_2 = 15$ m, thickness $t = 0.018$ m).

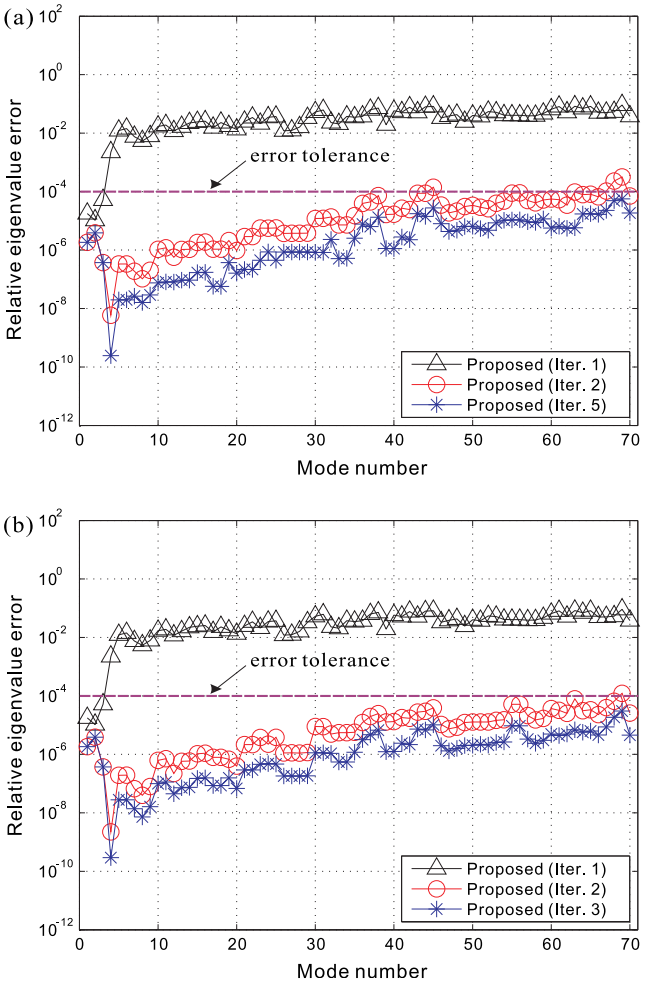

Fig. 9. Relative eigenvalue errors by the proposed method for the semi-submersible rig problem: (a) 1st, 2nd, and 5th iterations when $\bar{N}_b = 350$, (b) 1st, 2nd, and 3rd iterations when $\bar{N}_b = 600$.

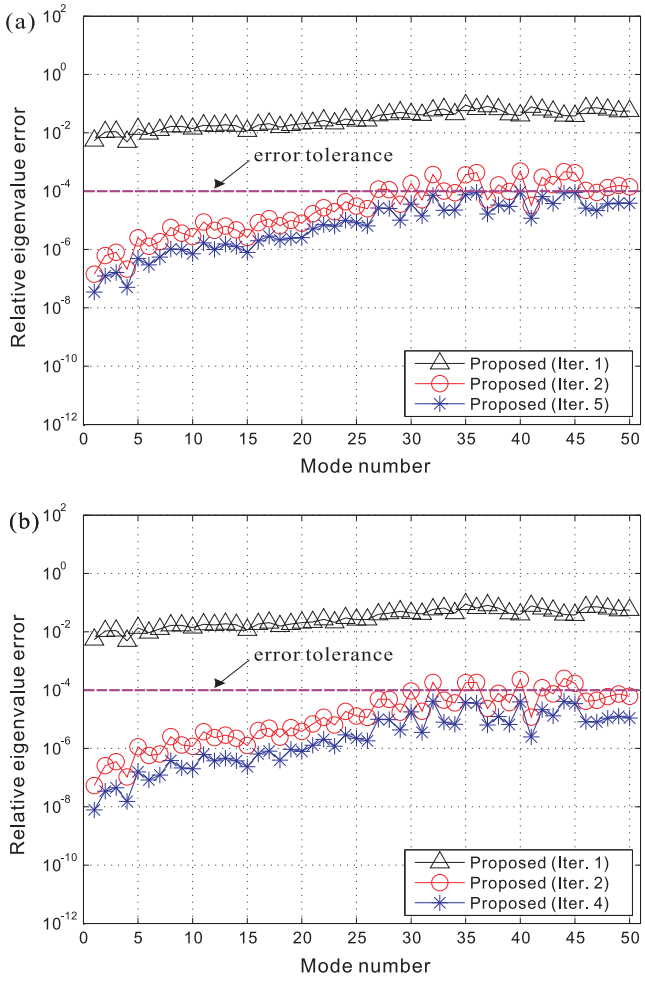

Fig. 11. Relative eigenvalue errors by the proposed method for the barge ship problem: (a) 1st, 2nd, and 5th iterations when $\bar{N}_b = 300$, (b) 1st, 2nd, and 4th iterations when $\bar{N}_b = 500$.

Table 6
Computational costs for the semi-submersible rig problem when $\bar{N}_b = 350$.

Items	Iteration counts	Computation times [sec]
IIRS	–	N/A
Proposed	5	247.07

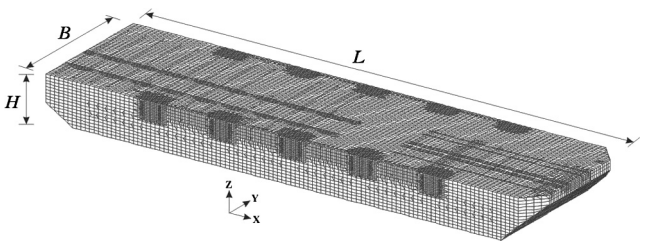

Fig. 10. Barge ship problem (26,688 shell elements, 157,368 DOFs, length $L = 140$ m, breadth $B = 12$ m, height $H = 37$ m, thickness $t = 0.025$ m).

Table 7
Computational costs for the barge ship problem when $\bar{N}_b = 300$.

Items	Iteration counts	Computation times [sec]
IIRS	–	N/A
Proposed	5	443.36

5. Conclusions

In this study, we developed the iterative algebraic dynamic condensation method. For the computing efficiency, the algebraic substructuring technique was employed. Using the procedures of the substructural stiffness condensation and the interface boundary reduction, the initial reduced model was calculated, and then, the iterative substructural inertial effect condensation was performed to find the final reduced model that satisfied the designated error tolerance. To verify the performance of the proposed method, several large structural FE models were tested. The numerical results showed that the proposed method outperformed the IIRS method in regards to solution accuracy and computational efficiency. Of particular significance, was that the proposed method could handle

large FE models that could not be handled at all using the IIRS method. Moreover, the computational efficiency of the proposed method was much superior to that of the IIRS method. This is because the formulation of the proposed method was expressed very efficiently with many small submatrices that were easier to compute.

In future work, it would be valuable to develop a more efficient iterative algebraic dynamic condensation method to solve FE models with more than several millions of DOFs. For this, it should be investigated whether the multi-level algebraic substructuring can be used with the proposed method.

Acknowledgements

This research was supported by a grant [MPSS-CG-2015-01] through the Disaster and Safety Management Institute funded by Ministry of Public Safety and Security of Korean government.

References

[1] Boo SH, Lee PS. A dynamic condensation method using algebraic substructuring. Intl J Numer Methods Eng 2016. http://dx.doi.org/10.1002/nme.5349.
[2] Guyan R. Reduction of stiffness and mass matrices. AIAA J 1965;3(2):380.
[3] Irons BM. Eigenvalue economisers in vibration problems. J R Aeronaut Soc 1963;67:526.
[4] Paz M. Dynamic condensation method. AIAA J 1984;22(5):724–7.
[5] O'Callanhan J. A procedure for an improved reduced system (IRS) model. In: Proceedings of the 7th international modal analysis conference, Bethel, CT.
[6] Suarez LE. Dynamic condensation method for structural eigenvalue analysis. AIAA J 1992;30(4):1046–54.
[7] Friswell MI, Garvey SD, Penny J. Model reduction using dynamic and iterated IRS techniques. J Sound Vib 1995;186(2):311–23.
[8] Xia Y, Lin R. A new iterative order reduction (IOR) method for eigensolutions of large structures. Intl J Numer Methods Eng 2004;59:153–72.
[9] Kidder RL. Reduction of structural frequency equations. AIAA J 1973;11(6):892.
[10] Henshell RD, Ong JH. Automatic masters from eigenvalues economization. Earthquake Eng Struct Dynam 1975;3:375–83.
[11] Ong JH. Improved automatic masters for eigenvalues economization. Finite Elem Anal Des 1987;3(2):149–60.
[12] John TS, Walter ST. Selection of component modes for flexible multibody simulation. AIAA J 1991;14(2):278–86.
[13] Papadimiriou C, Papadioti DC. Component mode synthesis technique for finite element model updating. Comput Struct 2013;126:15–28.
[14] Hou G, Maroju V. Component mode synthesis-based design optimization method for local structural modification. Struct Optim 1995;10:128–36.
[15] Lall S, Marsden JE, Glavaski S. A subspace approach to balanced truncation for model reduction of nonlinear control system. Int J Robust Nonlinear Control 2002;12(6):519–35.
[16] Mottershead JE, Friswell MI. Model updating in structural dynamics: a survey. J Sound Vib 1993;167(2):347–75.
[17] Kammer DC, Allen MS, Mayes RL. Formulation of an experimental substructure using a Craig-Bampton based transmission simulator. J Sound Vib 2015;359:179–94.
[18] Ibrahimbegovic A, Chen HC, Wilson EL, Taylor RL. Ritz method for dynamic analysis of linear systems with non-proportional damping. Int J Earthq Eng Struct Dyn 1990;19:877–89.
[19] Ibrahimbegovic A, Wilson EL. Automated truncation of Ritz vector basis in modal transformation. ASCE J Eng Mech Div 1990;116:2506–20.
[20] Ibrahimbegovic A, Taylor RL, Lim H. Nonlinear dynamics of flexible multibody systems. Comput Struct 2003;81:1113–32.
[21] Bathe KJ. Finite element procedures. USA: Prentice Hall; 1996.
[22] Hughes TJR. The finite element method: linear static and dynamic finite element analysis. Mineola, NY, USA: Dover; 2000.
[23] Bouhaddi N, Fillod R. A method for selecting master DOF in dynamic substructuring using the Guyan condensation method. Comput Struct 1992;45(5):941–6.
[24] Bouhaddi N, Fillod R. Substructuring using a linearized dynamic condensation method. Comput Struct 1992;45(4):679–83.
[25] Bouhaddi N, Fillod R. Substructuring by a two level dynamic condensation method. Comput Struct 1996;60(3):403–9.
[26] Kim HG, Cho MH. Improvement of reduction method combined with sub-domain scheme in large-scale problem. Intl J Numer Methods Eng 2007;70:206–51.
[27] Choi DS, Kim HG, Cho MH. Iterative method for dynamic condensation combined with substructuring scheme. J Sound Vib 2008;317(1–2):199–218.
[28] Baek SM. Study on the multi-level substructuring scheme and system condensation for the large-scaled structural dynamic analysis Ph.D. thesis. Department of Mechanical and Aerospace Engineering, Seoul National University; 2012.
[29] Hurty W. Dynamic analysis of structural systems using component modes. AIAA J 1965;3(4):678–85.
[30] Craig RR, Bampton MCC. Coupling of substructures for dynamic analysis. AIAA J 1968;6(7):1313–9.
[31] MacNeal RH. Hybrid method of component mode synthesis. Comput Struct 1971;1(4):581–601.
[32] Benfield WA, Hruda RF. Vibration analysis of structures by component mode substitution. AIAA J 1971;9:1255–61.
[33] Kuhar EJ, Stahle CV. Dynamic transformation method for modal synthesis. AIAA J 1974;12(5):672–8.
[34] Rubin S. Improved component-mode representation for structural dynamic analysis. AIAA J 1975;13(8):995–1006.
[35] Craig RR, Hale AL. Block-Krylov component synthesis method for structural model reduction. AIAA J 1988;11(6):562–70.
[36] Bourquin F. Component mode synthesis and eigenvalues of second order operators: discretization and algorithm. Math Model Numer Anal 1992;26 (3):385–423.
[37] Boo SH, Kim JG, Lee PS. A simplified error estimator for the Craig-Bampton method and its application to error control. Comput Struct 2016;164:53–62.
[38] George A. Nested dissection of a rectangular finite element mesh. SIAM J Numer Anal 1973;10(2):345–63.
[39] Hendrickson B, Rothberg E. Effective sparse matrix ordering: just around the bend. In: Proceedings of eighth SIAM conference on parallel processing for scientific computing, Minneapolis, Minnesota.
[40] Yang C, Gao W, Bai Z, Li XS, Lee LQ, Husbands P. E. NG. An algebraic substructuring method for large-scale eigenvalue calculation. SIAM. J Sci Comput 2005;27(3):873–92.
[41] Kaplan MF. Implementation of automated multi-level substructuring for frequency response analysis of structures Ph.D. thesis. Austin, TX: Department of Aerospace Engineering & Engineering Mechanics, University of Texas at Austin; 2001.
[42] Bennighof JK, Lehoucq RB. An automated multilevel substructuring method for eigenspace computation in linear elastodynamics. SIAM J Sci Comput 2004;25 (6):2084–106.
[43] Boo SH, Kim JG, Lee PS. Error estimation method for automated multi-level substructuring method. Intl J Numer Methods Eng 2016;106:927–50.
[44] Dvorkin EN, Bathe KJ. A continuum mechanics based four-node shell element for general nonlinear analysis. Eng Comput 1984;1(1):77–88.
[45] Lee PS, Bathe KJ. Development of MITC isotropic triangular shell finite elements. Comput Struct 2004;82(11–12):945–62.
[46] Lee YG, Lee PS, Bathe KJ. The MITC3+ shell finite element and its performance. Comput Struct 2014;138:12–23.
[47] Karypis G, Kumar V. METIS v4.0, a software package for partitioning unstructured graphs, partitioning meshes, and computing fill-reducing orderings of sparse matrices. Technical report, University of Minnesota, Minneapolis, MN; 1998.